THE UNIVERSITY OF MICHIGAN

COLLEGE OF ENGINEERING
Department of Engineering Mechanics
Department of Mechanical Engineering

Tire and Suspension Systems Research Group

Technical Report No. 11

MEASUREMENT OF AIRCRAFT TIRE MECHANICAL PROPERTIES USED IN SHIMMY ANALYSIS BY MEANS OF SCALE MODELS

G. H. Nybakken
R. N. Dodge
S. K. Clark

ORA Project 05608

supported by:

NATIONAL AERONAUTICS AND SPACE ADMINISTRATION
GRANT NO. NGL 23-005-010
WASHINGTON, D.C.

administered through:

OFFICE OF RESEARCH ADMINISTRATION ANN ARBOR

September 1970

TABLE OF CONTENTS

LIST OF ILLUSTRATIONS

LIST OF ILLUSTRATIONS (Concluded)

NOMENCLATURE

English Letters

C - couple or moment

D - tire nominal diameter

F - force on tire

ℓ - contact patch half length

p_o - tire inflation pressure

q - pneumatic trail

w - tire section width

Greek Letters

δ - tire deflection

λ - tire relaxation length

η - tire damping coefficient

ψ - yaw angle or angle of rotation of tire about a vertical, or steer, axis

Subscripts

x, y, z - coordinate directions according to Figure 1

ψ - direction normal to yaw direction

E - energy

F - force

I. INTRODUCTION

Current research activities at The University of Michigan have been directed toward demonstrating the validity of small scale modeling of aircraft tires, as has recently been reported by Dodge, Lackey, Nybakken, and Clark [1]. Theoretical investigations lead one to believe that such small scale modeling can be satisfactorily achieved, at least in theory, for all of the mechanical properties of aircraft tires including static, rolling, and dynamic conditions. Methods have been developed for the manufacture of such small scale models and for determining their mechanical properties. The previously cited reference shows excellent agreement between full size static tire stiffness properties and those measured on small scale models, referred to a common dimensionless basis.

The next step of increasing complexity in this program is to attempt to verify such modeling concepts for the case of the rolling tire under steady state conditions. This can be accomplished by measuring the proper mechanical characteristics of small scale tires under such conditions and comparing these with known results from full size prototypes.

Six specific tire mechanical properties are chosen in this study for measurement on small scale tires and for comparison with data from the full size prototypes. These properties were chosen as those which are important in shimmy analysis, since the general thrust of this research program is to determine as a next step, subsequent to the work reported here, these properties as influenced by high rolling speed and by transient dynamic conditions.

For that reason it was felt advisable to concentrate on tire mechanical properties which would have immediate application to shimmy analysis. The influence of dynamic effects on these properties would then give some indication as to the inaccuracy of statically determined tire stiffness data such as is currently used in shimmy predictions.

II. SUMMARY

The theory of tire modeling has recently been outlined in Ref. [1]. It was shown there that small scale tires, built in accordance with proper dimensionless concepts, exhibit static mechanical properties which agree well with those found on full size aircraft tires of the same design, expressed on a dimensionless basis. The data presented in this report shows that this same modeling concept can be satisfactorily extended to tire mechanical properties observed under steady state slow-rolling conditions. This conclusion is based on the results of comparisons of six basic tire mechanical characteristics commonly used in landing gear shimmy analysis.

Experiments have been conducted on small scale models of a 40 x 12, 14 PR, Type VII aircraft tire, using a scale factor of 8.6. These experiments cover the following six tire mechanical properties:

(a) tire contact patch half length, ℓ

(b) tire lateral spring rate, k_y

(c) tire lateral damping coefficient, η_y

(d) yawed-rolling relaxation length, λ_y

(e) self aligning torque, C_z

(f) pneumatic trail, q

The first three of these properties are basically static in nature and usually are obtained on a non-rolling tire. The last three properties require the tire to be rolled in order to be measured, and hence are intimately tied to the rolling process. Generally speaking, agreement between model tire

mechanical characteristics and those measured on the full size aircraft tire is good. However, in the case of the rolling tire properties agreement is more satisfactory at low slip angles than at higher ones. This is because it is difficult to accurately produce in small scale the concrete runway surface on which the original prototype aircraft tire was taken, and points up the importance of the roadway surface in the measurement of mechanical tire characteristics.

III. MECHANICAL PROPERTIES OF MODEL AND PROTOTYPE TIRES

Previous work has shown that dimensionless structural modeling of an aircraft tire can only be assured if certain dimensionless quantities are the same in both model and prototype. In order to assure a comparable basis for comparison of data, the following dimensionless variables are used in discussing the mechanical properties measured in this report:

(a) The tire contact patch half length is expressed by the dimensionless ratio ℓ/D, where D is the tire characteristic length, in this case the outside tire diameter.

(b) Lateral load-lateral deflection characteristics of the tire are expressed by the relationship between (F_y/p_oD^2) and (δ_y/D).

(c) Lateral damping coefficient η_y is by definition dimensionless.

(d) Yawed-rolling relaxation length λ_y/D.

(e) Self-aligning torque (C_z/p_oD^3) vs. ψ.

(f) Side force (F_ψ/p_oD^2) vs. ψ.

(g) Pneumatic trail (q/D) vs. ψ.

A coordinate system for the tire is shown in Figure 1.

In addition to establishing appropriate dimensionless variables, the modeling concept discussed in Ref. [1] also gives a technique for establishing proper inflation and load conditions for the model tires. This process is based on the relationship between the fore-aft stiffness characteristics of the model tire and its carcass modulus of elasticity. Pressure and load

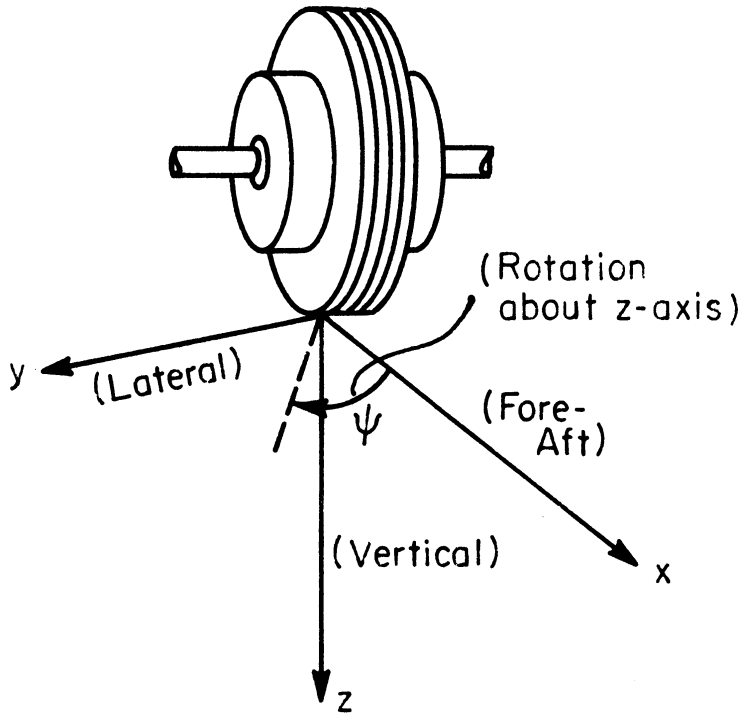

Figure 1. Tire coordinate directions.

conditions for the model tires obtained through the use of this technique are listed in Table I, as is the rated load and pressure for the 40 x 12 prototype tire.

TABLE I

TIRE OPERATING CONDITIONS

Tire	p_o (psi)	F_z (lb)	D (in.)	w* (in.)
40 x 12 - 14 PR Type VII Prototype	95	14500	39.3	12.12
Model A-18 (2 Ply, 840/2 Nylon, 10 EPI)	25	48.2	4.57	1.67
Model A-15 (2 Ply, 840/2 Nylon, 10 EPI)	23	48.2	4.58	1.66
Model A-14 (2 Ply, 840/2 Nylon, 10 EPI)	19	38.2	4.58	1.64
Model A-13 (2 Ply, 840/2 Nylon, 10 EPI)	20	38.2	4.56	1.62

*w = Section Width

Experimental data for the 40 x 12 prototype tire used for comparison in this report was taken from the work of Horne and Smiley [2].

Summaries of the comparisons of the six tire mechanical properties previously discussed, measured on four different model tires, with the full size data taken from 40 x 12 tire are shown in Figures 2 through 8. The model tires used for these measurements were previously used in determining the static properties in Ref. [1].

The tire contact patch half length is shown for the model and full size tires in Figure 2. This is a static tire property and generally the model tires tested show contact patch lengths which agree well with the full size tire, the variation between model tires probably being due to minor structural variations.

The second tire property, as shown in Figure 3, is the lateral spring rate of the tire. This also exhibits good agreement between model and prototype data, and was previously used in Ref. [1]. It is repeated here since it is a characteristic tire mechanical property which is quite important in shimmy analysis.

A tire mechanical property which is also quite important in shimmy analysis is the tire lateral damping coefficient. Two comparisons between model and prototype tires for this property are shown in Figures 4 and 5. As can be seen, the agreement is very good in Figure 4, where the lateral damping coefficient is defined as the ratio of the maximum half-height of the corresponding force-deflection hysteresis loop to the maximum total force, as defined by Horme and Smiley [2]. The agreement is also good in Figure 5,

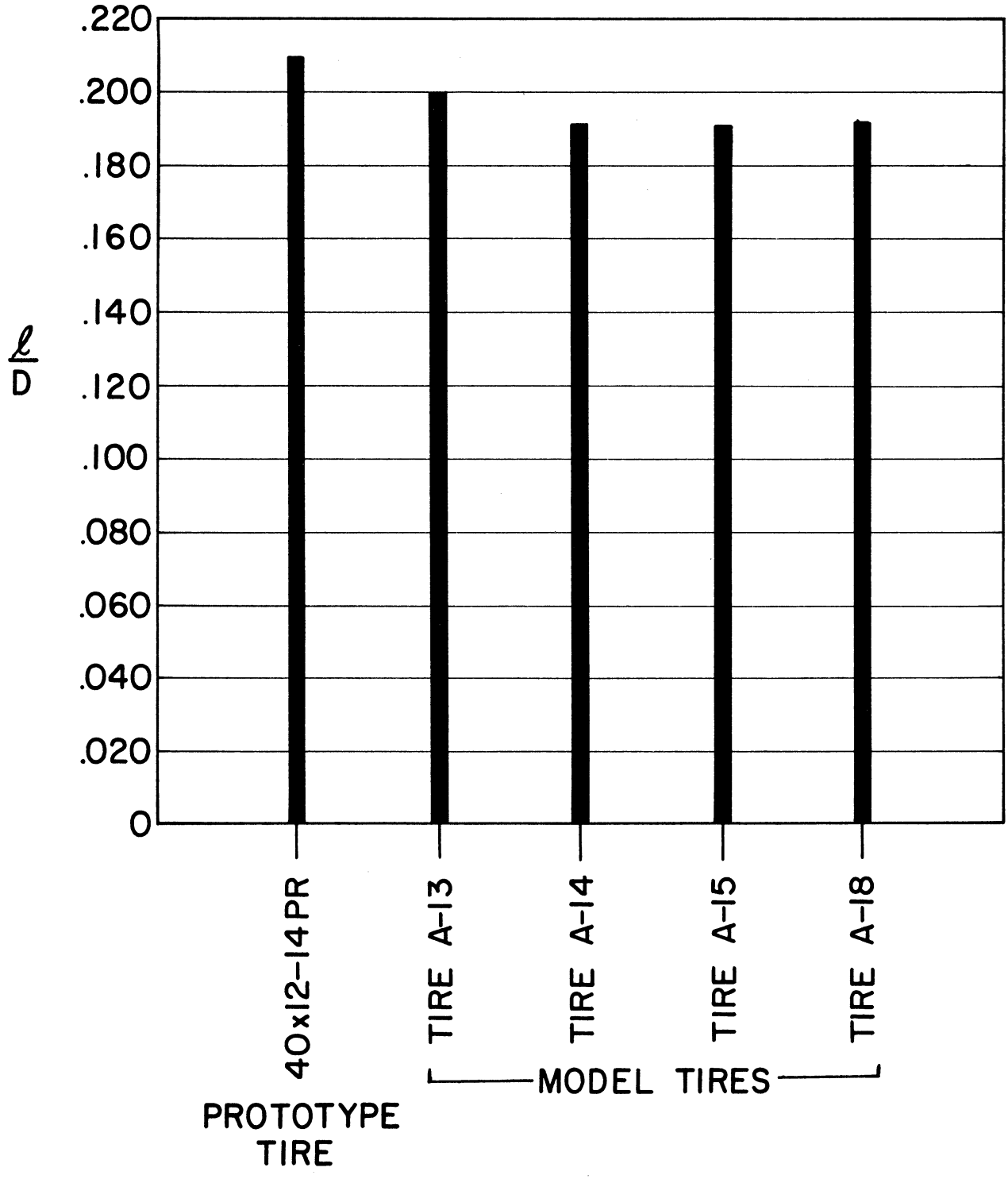

Figure 2. Tire half contact-patch length data for model and prototype tires.

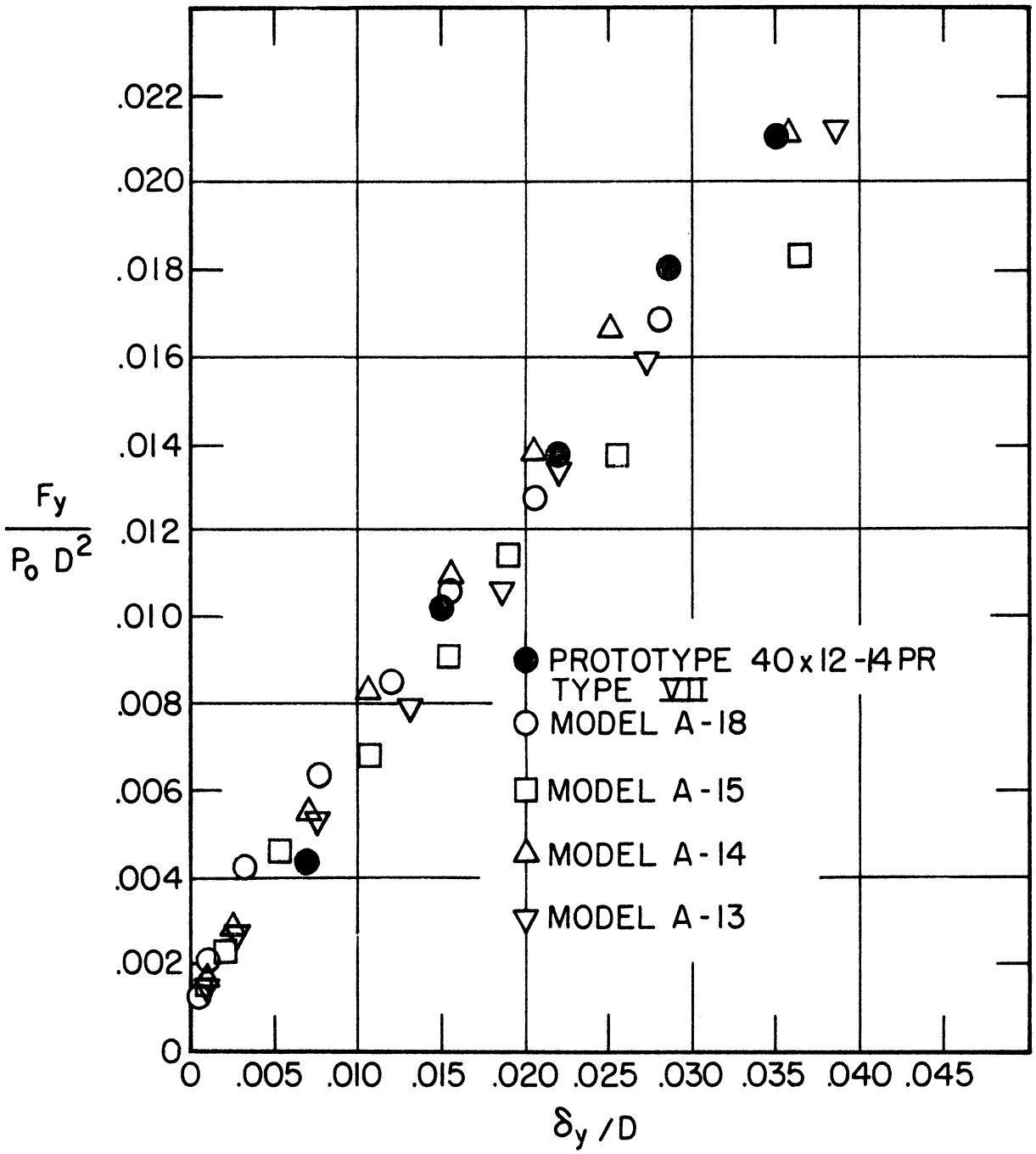

Figure 3. Lateral load-lateral deflection data for model and prototype tires.

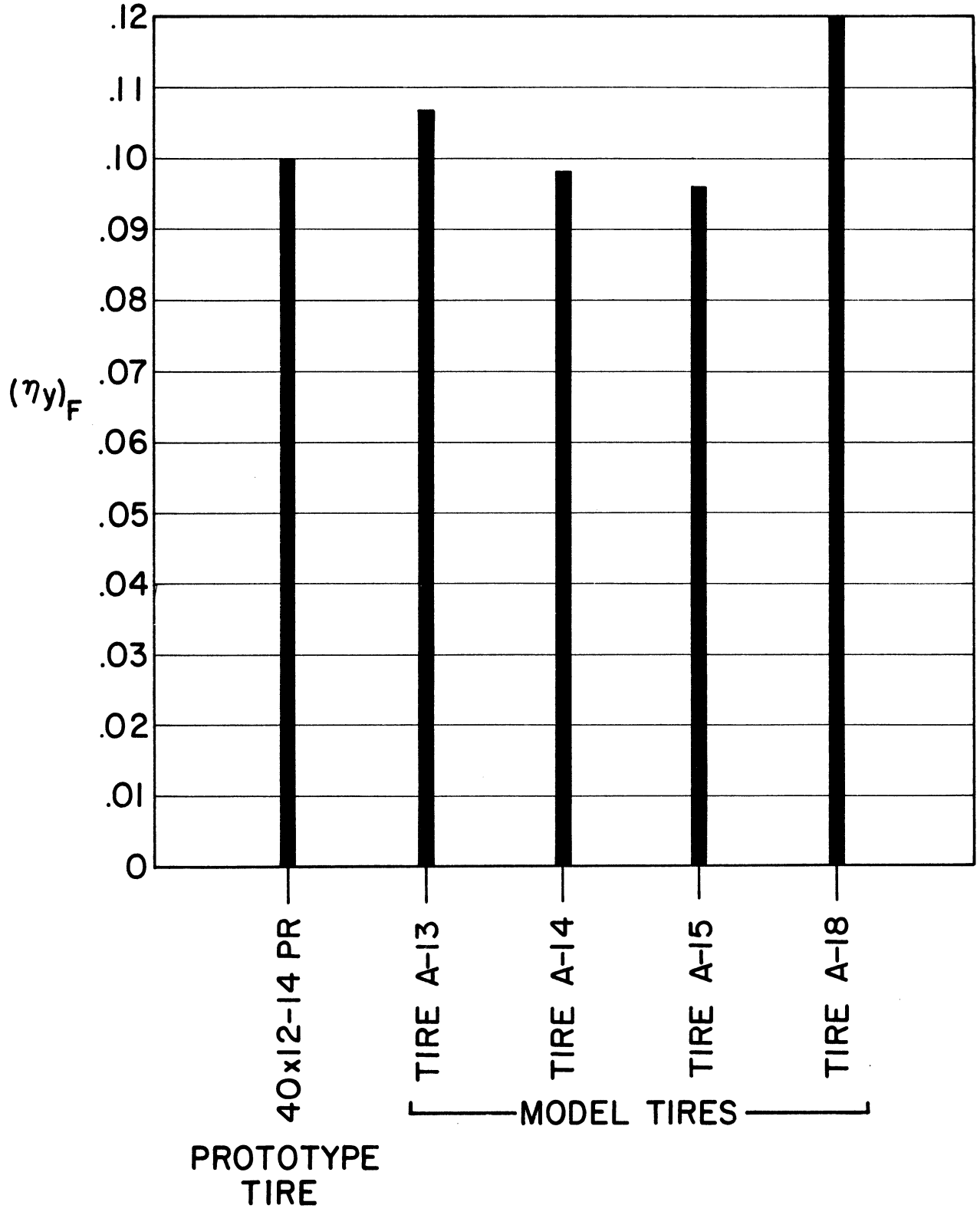

Figure 4. Lateral damping coefficient data for model and prototype tires, $(\eta_y)_F$ based on force ratio.

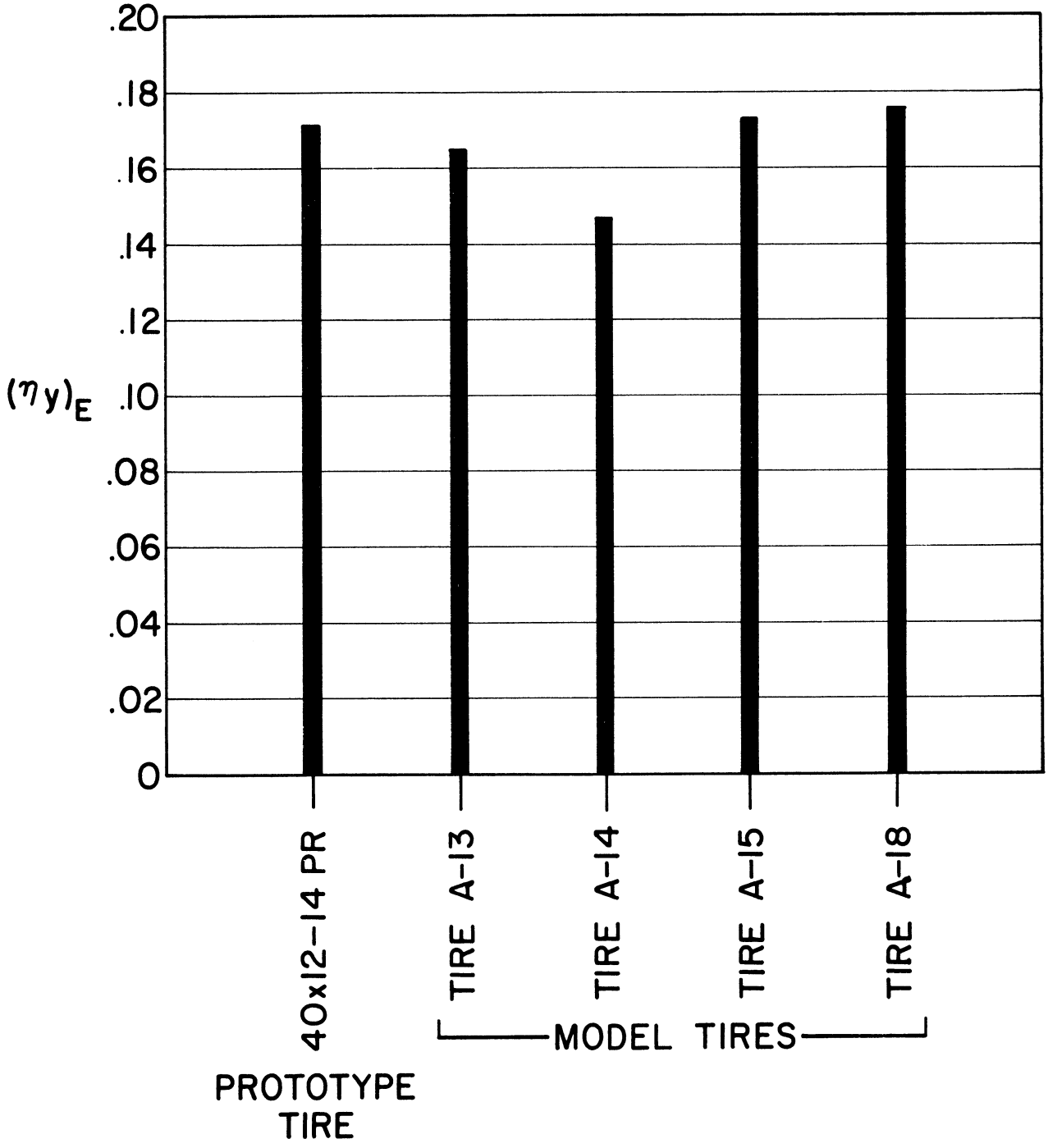

Figure 5. Lateral damping coefficient data for model and prototype tires, $(\eta_y)_E$ based on energy ratio.

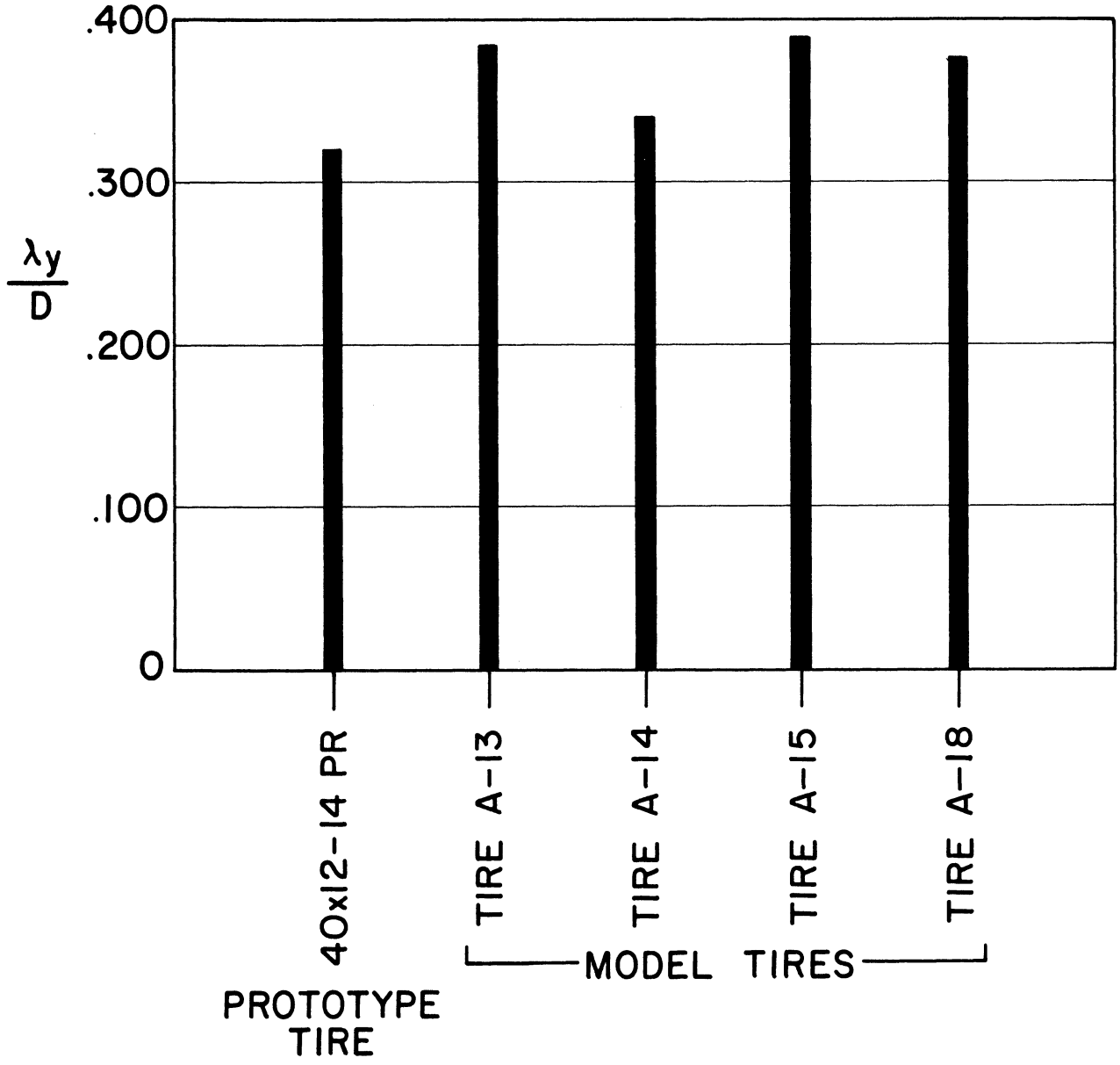

Figure 6. Yawed-rolling relaxation length data for model and prototype tires.

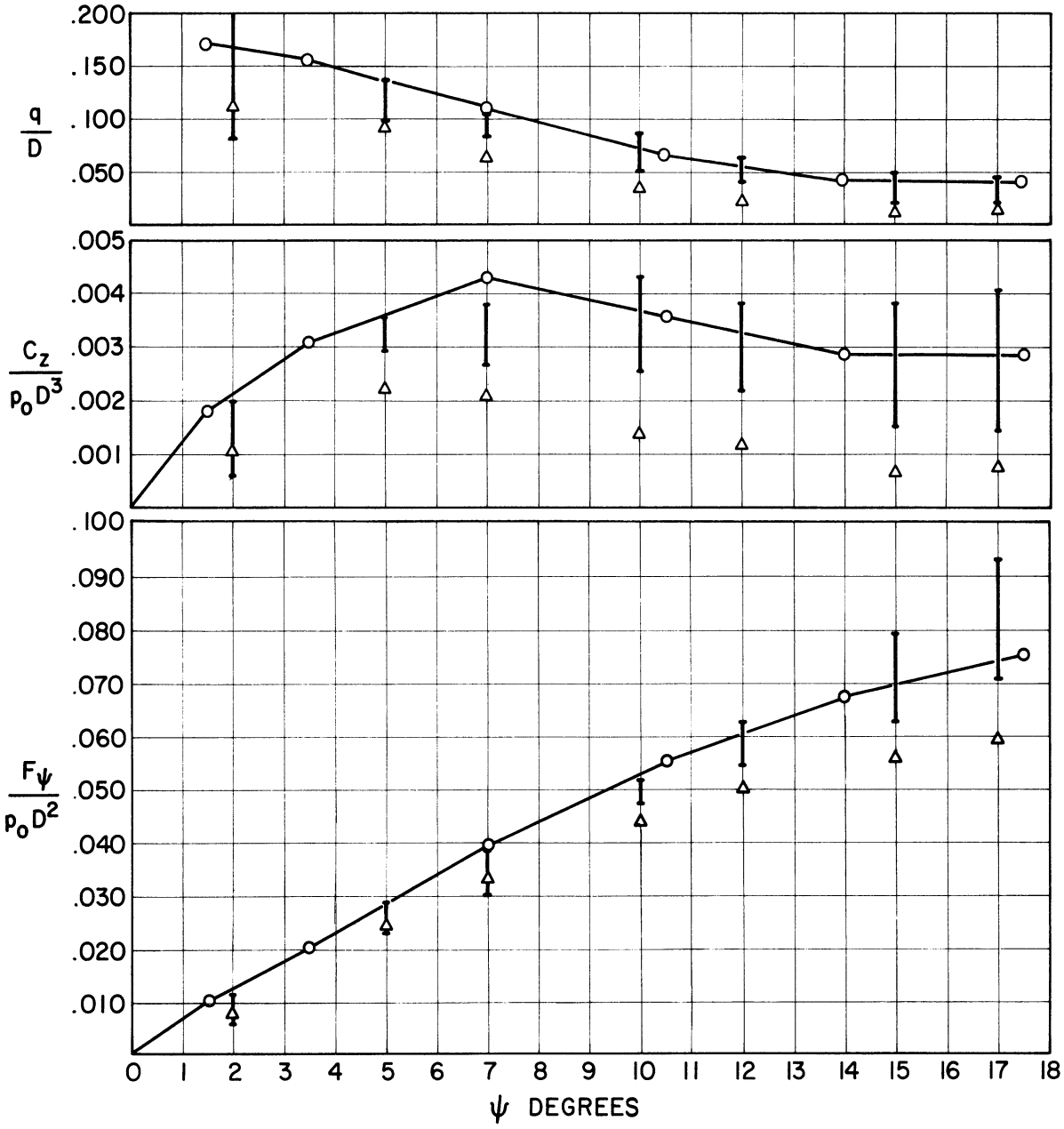

Figure 7. Side force, self-aligning torque and pneumatic trail data for model and prototype tires. Surface No. 9.

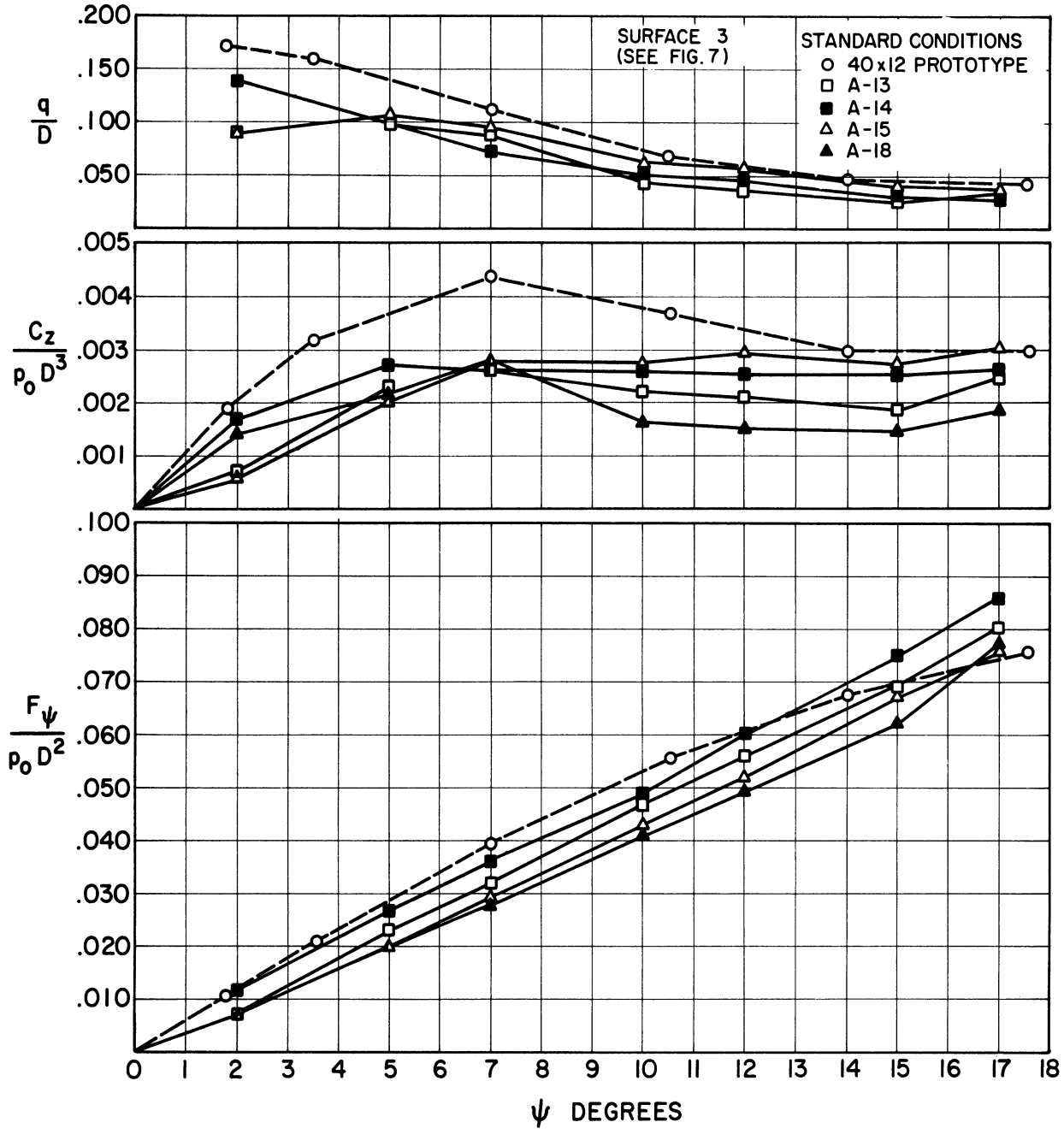

Figure 8. Normal side force, self-aligning torque and pneumatic trail data for model and prototype tires. Surface No. 10.

where the lateral damping coefficient is alternately defined as the ratio of the energy loss per cycle to the energy contained in the area beneath the loading portion of the load-deflection curve.

An important tire rolling property used in shimmy analysis is the yawed-rolling relaxation length. This is defined as the distance a yawed tire must roll to produce a side force equal to (1 - 1/e) of the maximum side force developed at the steady-state steer angle condition. A comparison of such measurements on the model tires with those taken on the prototype is shown in Figure 6. Again, agreement is good between the two sets of data.

There are two additional tire mechanical properties important to shimmy analysis which require a rolling tire for their definition. They are tire side force and self-aligning torque caused by operating the tire at various slip angles. These two properties were measured for the model tires used here, and from this measured data the pneumatic trail was gotten by taking the ratio of self-aligning torque to side force for a particular set of conditions. All three of these properties are presented in the subsequent graphs.

One important characteristic of these three tire properties is immediately evident. This is their strong dependence on the type of surface on which the tire rolls. A total of ten surfaces were used in the experimental measurement of side force and self-aligning torque. The range of values gotten from these tests is shown in Figure 7, where it is seen that the spread of data is quite significant, and illustrates a strong influence of surface conditions. Generally the full size prototype tire data lies inside the ranges shown, with the exception of the peak self-aligning torque. This is possibly lower in

these model tests since they were done against a cylindrical roadwheel, while the prototype data was taken on the runway. Our contact patch will generally be somewhat shorter and our pressure distribution somewhat less favorable for developing peak self-aligning torque than the flat runway surface.

Figure 8 shows this data for four model tires, and for the prototype tire, for a specific roadwheel surface. There is some variation among the model tires due to structural differences, particularly in the self-aligning torque. However, this surface is not particularly the best one for model tire mechanical measurements, and "sharper" surfaces, with more asperities, may tend to reduce this scatter.

This entire comparison represents an interesting and we feel fruitful observation, applicable in general to the determination of tire mechanical properties, since it seems to indicate that different observers and experimenters can only expect complete agreement between tire mechanical property data taken on identical runway surfaces. This clearly has application to cooperative testing programs where various agencies participate.

IV. MEASUREMENT OF TIRE MECHANICAL PROPERTIES

STATIC PROPERTIES

Model tire footprints were taken by the usual ink and paper method at standard conditions of inflation pressure and vertical load. The contact length was measured from the footprint. Figure 9 shows a typical footprint.

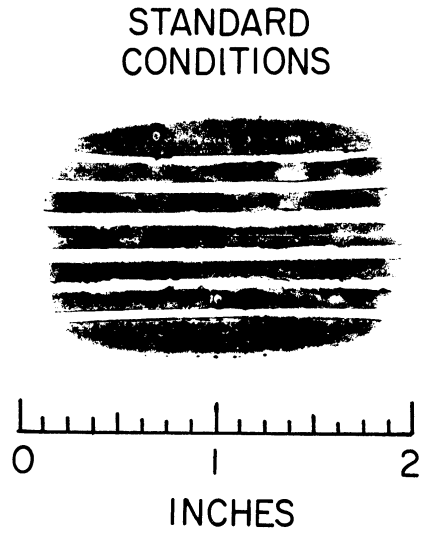

Figure 9. Typical model tire footprint.

Lateral stiffness data was taken on the static testing device described in Ref. [1].

Lateral damping cycles were taken on the apparatus shown in Figures 10 and 11. Thus apparatus basically consists of the static testing device discussed in Ref. [1]. Here the lateral force is generated by a lead screw and transmitted through a strain ring force-transducer to the movable plate. The plate rests on three steel balls and translates with almost no friction. The plate displacement relative to the run of the tire is measured by a LVDT inserted between the tire yoke and the plate. Both displacement and force

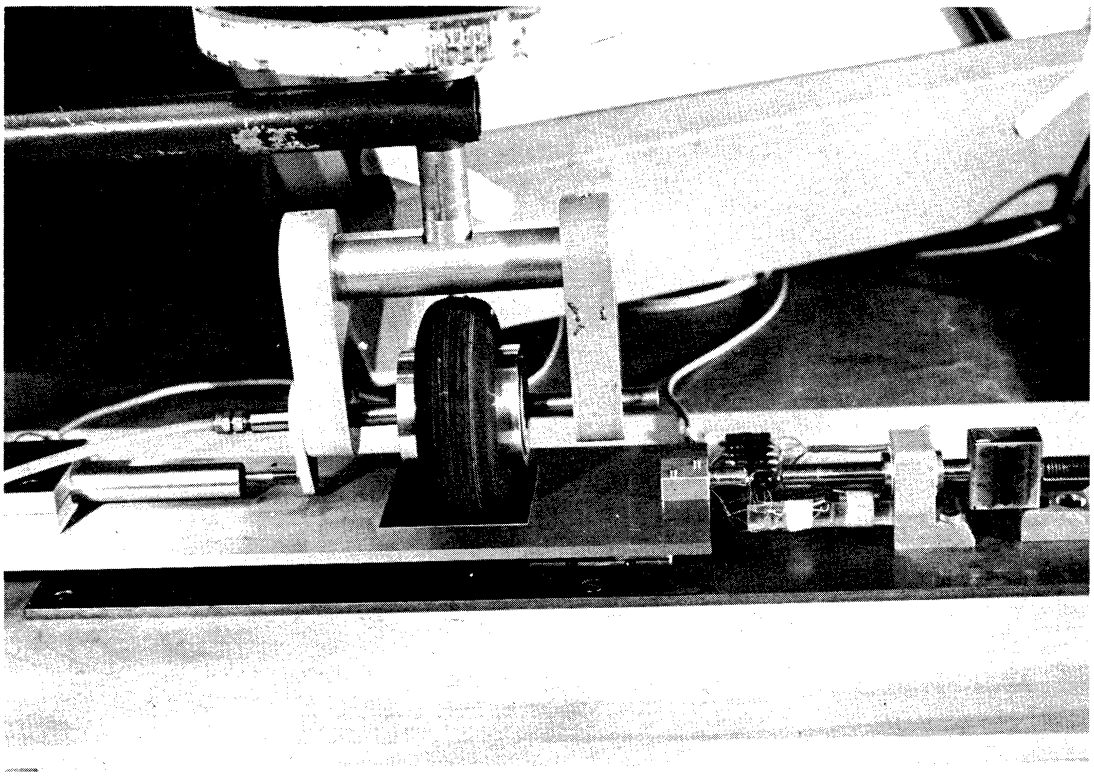

Figure 10. Components of lateral damping test apparatus.

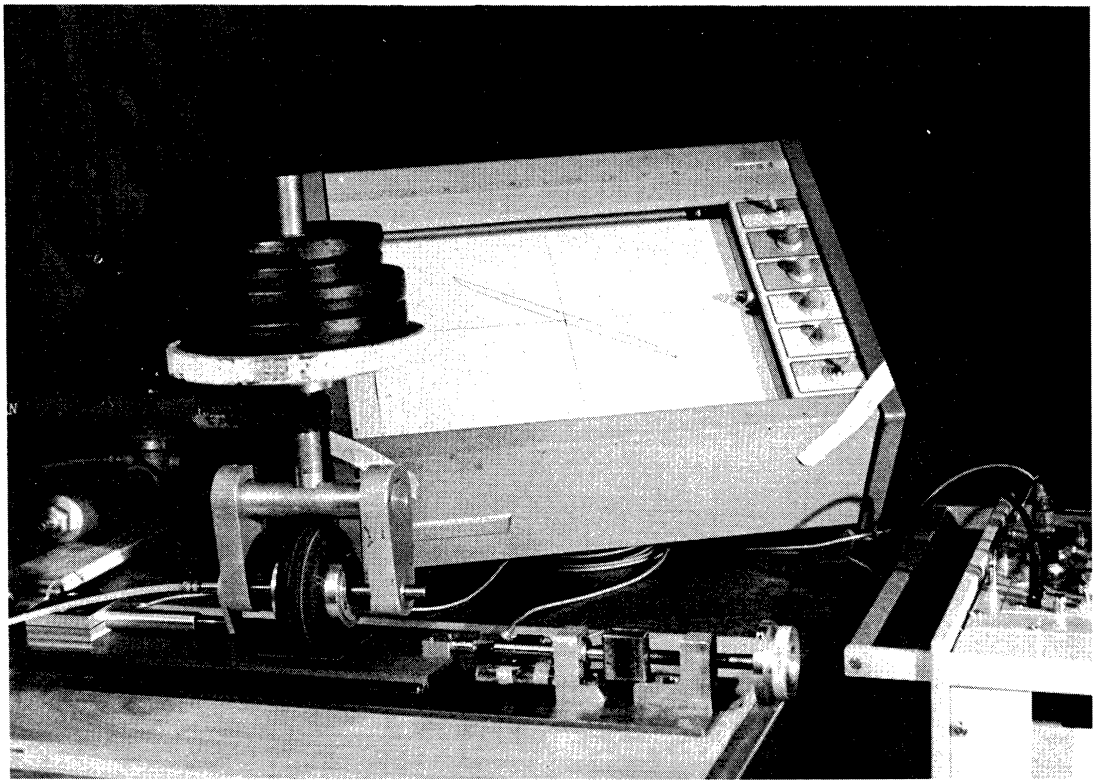

Figure 11. Lateral damping test apparatus.

signals are fed into Sanborn carrier amplifiers with the outputs of the amplifiers going into an X-Y recorder. Figure 10 shows the movable plate, tire and transducers. Figure 11 shows an overall view of the testing machine, Sanborn recorder and amplifiers and the X-Y recorder.

A typical lateral hysteresis loop is shown in Figure 12. Because of the dimensionless nature of most damping coefficients, no scales are needed for the axes. One definition of a lateral damping factor, used by Smiley and Horne [2], is the ratio of the maximum half-height of the force-deflection hysteresis loop to the maximum total force. Referring to Figure 12, $(\eta_y)_F$ is equal to the ratio A/B of the forces. Another definition of damping factors is based on energy or area measurements. The definition used in the preceding section is the ratio of the energy loss per cycle to the energy per cycle defined by the triangular area under the top curve. Referring to Figure 12, $(\eta_y)_E$ is equal to the ratio of the areas $\Delta E/E$.

SLOW ROLLING PROPERTIES

The slow rolling tests were performed on a 30-in. diameter, 4-in. wide cast iron roadwheel. Different adhesive surface are attached to the polished cast iron surface to simulate different roadways. The tire and rim assembly are mounted in a yoke such that forces normal to the plane of the wheel and moments about the vertical axis can be measured. The yoke is mounted in bearings attached to the end of a horizontal hinged arm, so that the whole assembly can easily be swung up off the roadwheel and out of contact. The roadwheel, yoke and arm are shown in Figure 13. The normal or side force, F_ψ, is measured by a strain ring force transducer shown in Figure 14. The

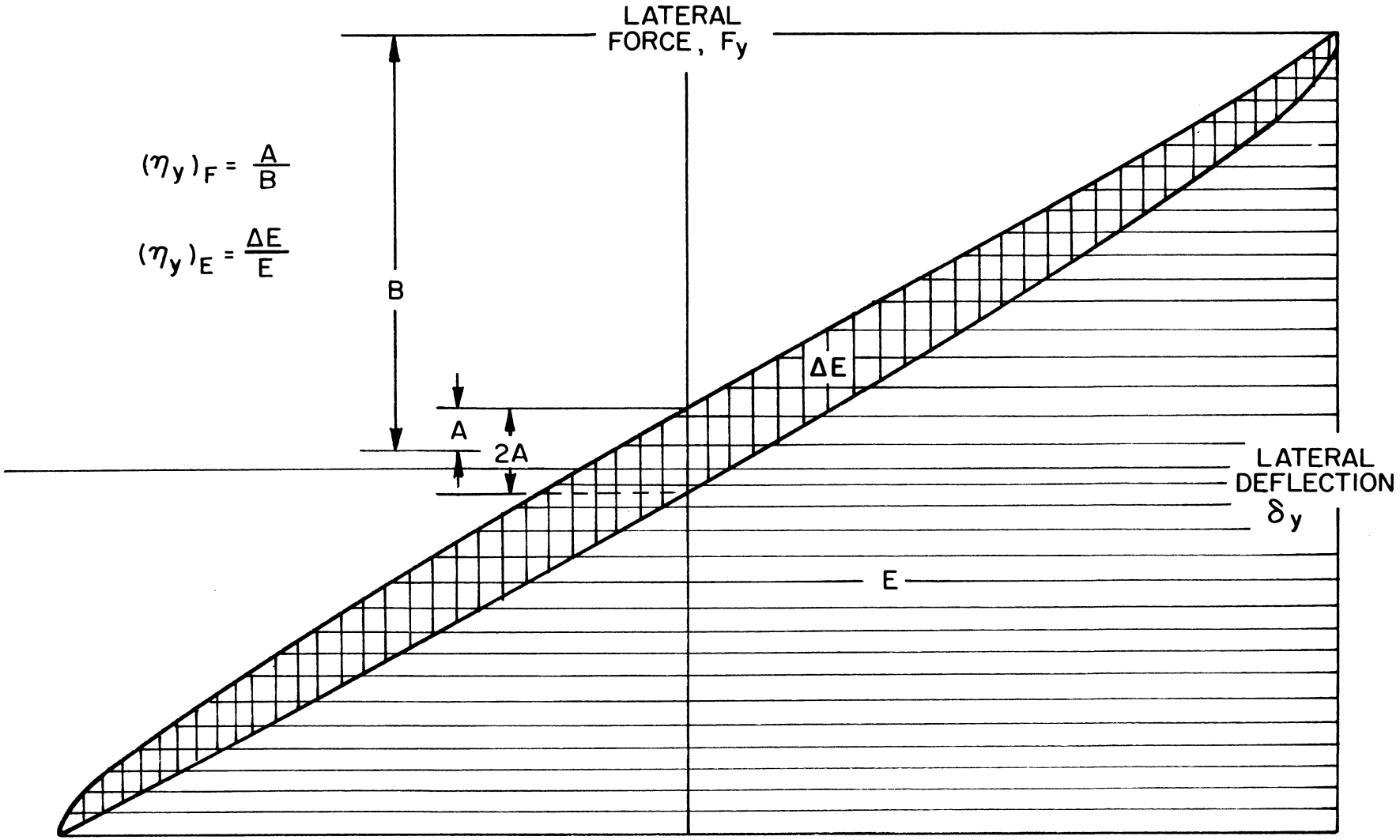

Figure 12. Typical lateral hysteresis curve.

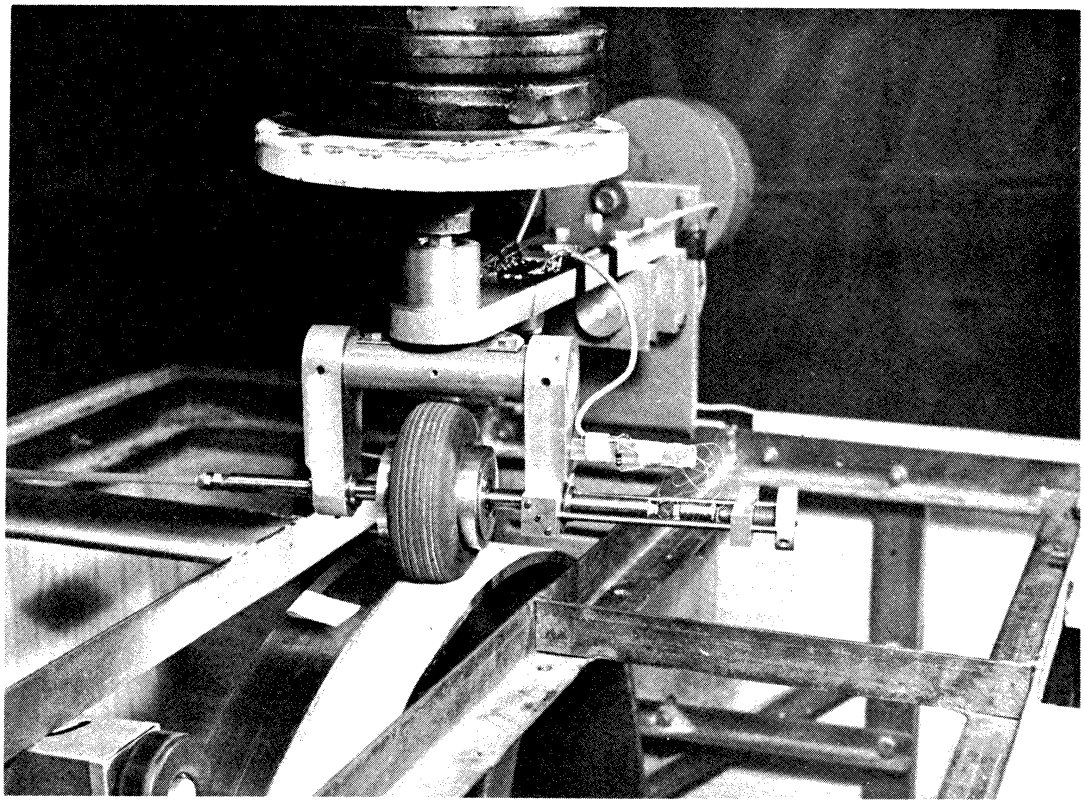

Figure 13. Model tire roadwheel, yoke and arm assembly.

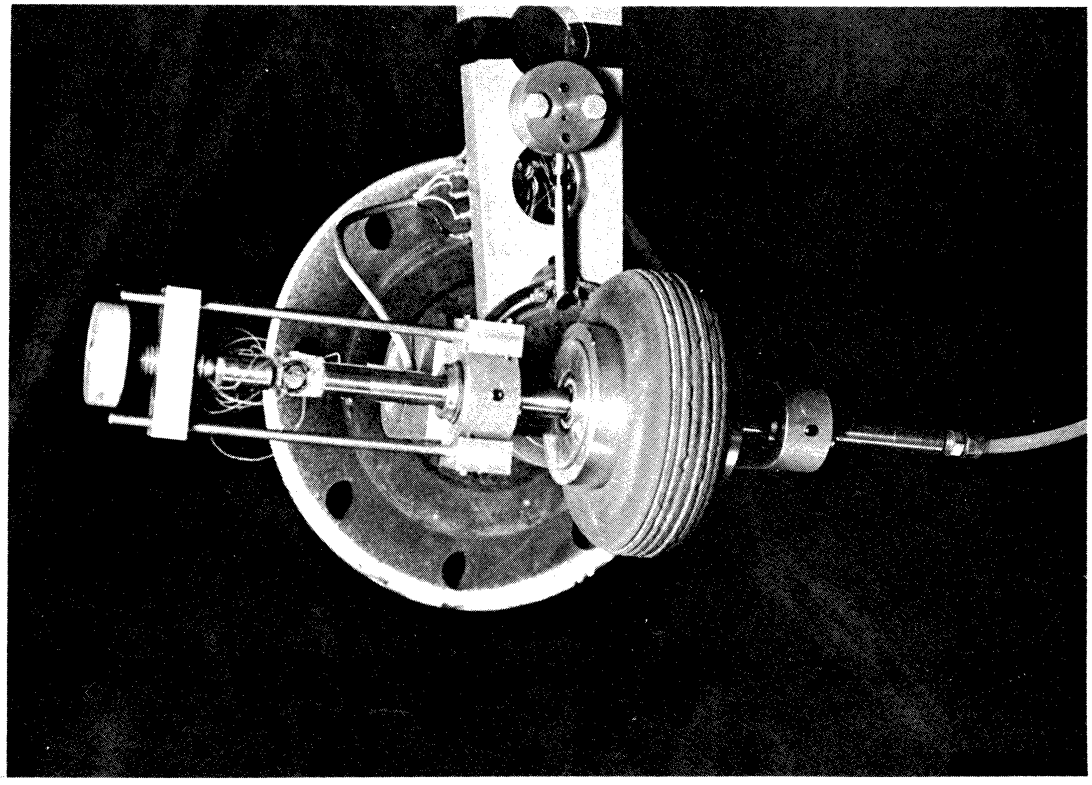

Figure 14. Transducers for measuring side force and self-aligning torque.

model wheel bearings are mounted in the rim so that the non-rotating axles can be mounted in linear ball bushings and attached to the force transducer. The force transducer butts against a rigid harness attached to the yoke and measures side force perpendicular to the wheel plane. The torque about the vertical, C_Z, is measured by a drag link transducer shown in Figure 14. The yoke is mounted in ball bearing to allow rotation about the vertical axis. A drag link with a built-in end at the arm and a pin joint at the yoke is instrumented with strain gages. The pin joint is attached to a slider which can be clamped at the desired yaw angle.

Relaxation length, λ_y, was measured by placing the tire at a yaw angle, rotating the roadwheel one tire contact length and measuring the side force build-up. The roadwheel displacement is measured by a precision potentiometer circuit. The tire side force measurement is accomplished by the strain ring. Both roadwheel displacement and side force are recorded by an X-Y plotter, as shown in Figure 15.

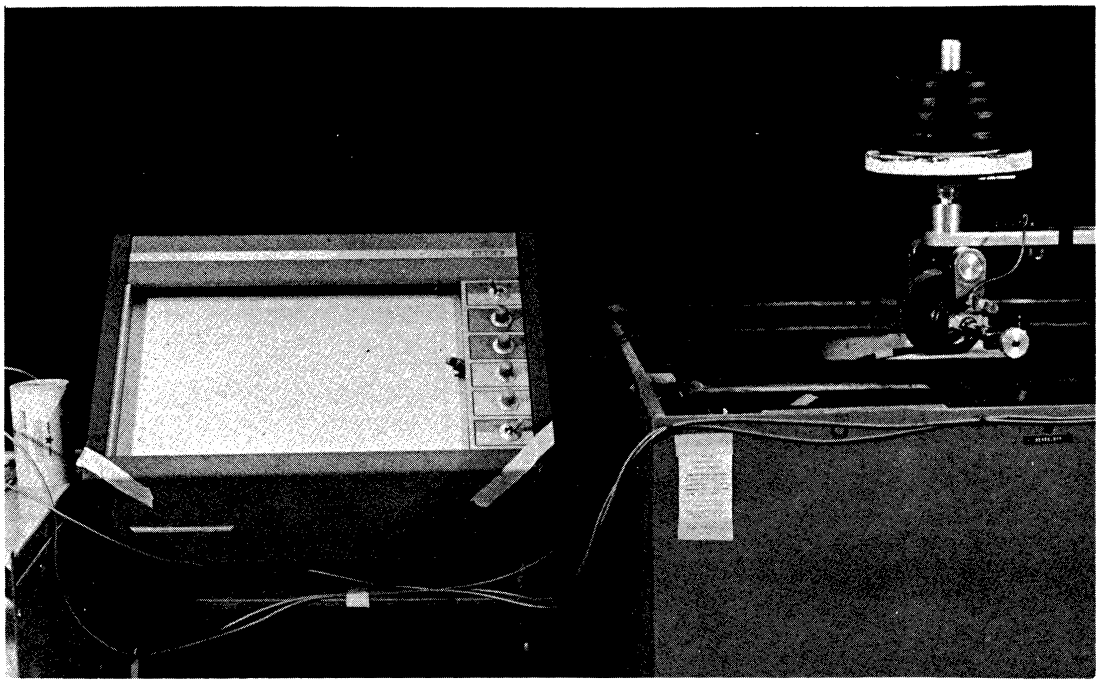

Figure 15. Yawed-rolling relaxation-length test apparatus.

Figure 16 shows a typical side force build-up curve obtained by this system. The tire rotates one contact length, 2ℓ, the axle and force transducer rest against the rigid harness and the side force build-up is recorded. The first horizontal slope is taken as the maximum side force. Variations after this point are due to maximum side force variation around the circumference of the tire. As shown in Figure 16, the maximum amplitude A is multiplied by $(1 - 1/e) = .632$. The distance the tire rolls to produce a side force of .632A is the measured relaxation length, λ_y. A few tests using self-aligning torque in place of side force gave basically the same relaxation lengths.

Three other slow rolling quantities were measured on a steady state basis. Side force, F_ψ, self-aligning torque, C_Z, and pneumatic trail, $q = C_Z/F_\psi$, were measured while the roadwheel was rotated by hand at a speed of about 0.8 ft/sec. Figure 13 shows the test in progress. An individual procedure for finding zero yaw angle was used on each tire, and allowed it to be located to within 1/4°. Once zero yaw angle is known, the tire was run at increasing yaw angles while the steady state values of F_ψ and C_Z, were recorded on an oscillograph. Variations in these quantities, which at small yaw angles could be very significant, were usually due to circumferential tire structure variation and difference in tire mounting. To eliminate the effect of these variations, the average value was computed using three measurements taken in one direction of rolling. Then the tire was dismounted, turned around and the procedure duplicated. Then averages of both sides of the tire were averaged together to get the values used in the preceding section. Figure 17 shows

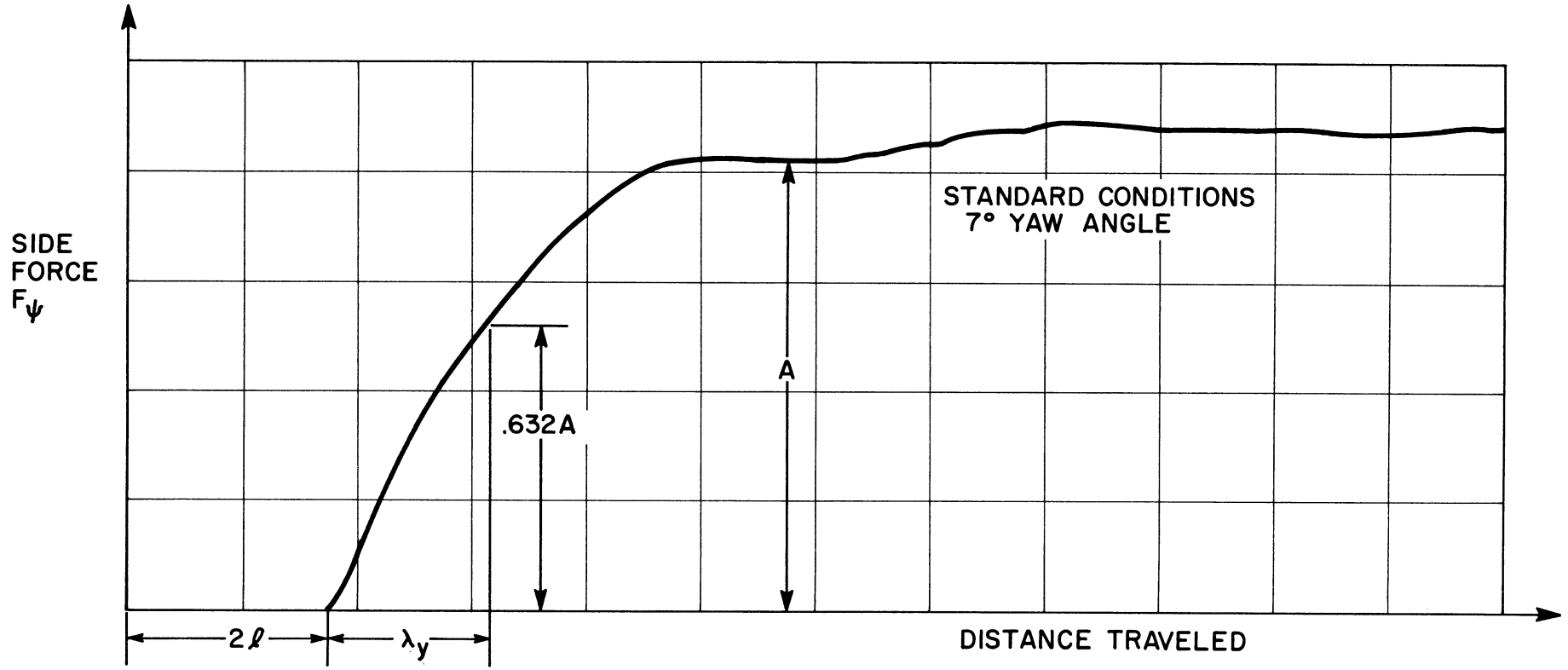

Figure 16. Typical data and data reduction for determining yawed-rolling relaxation length.

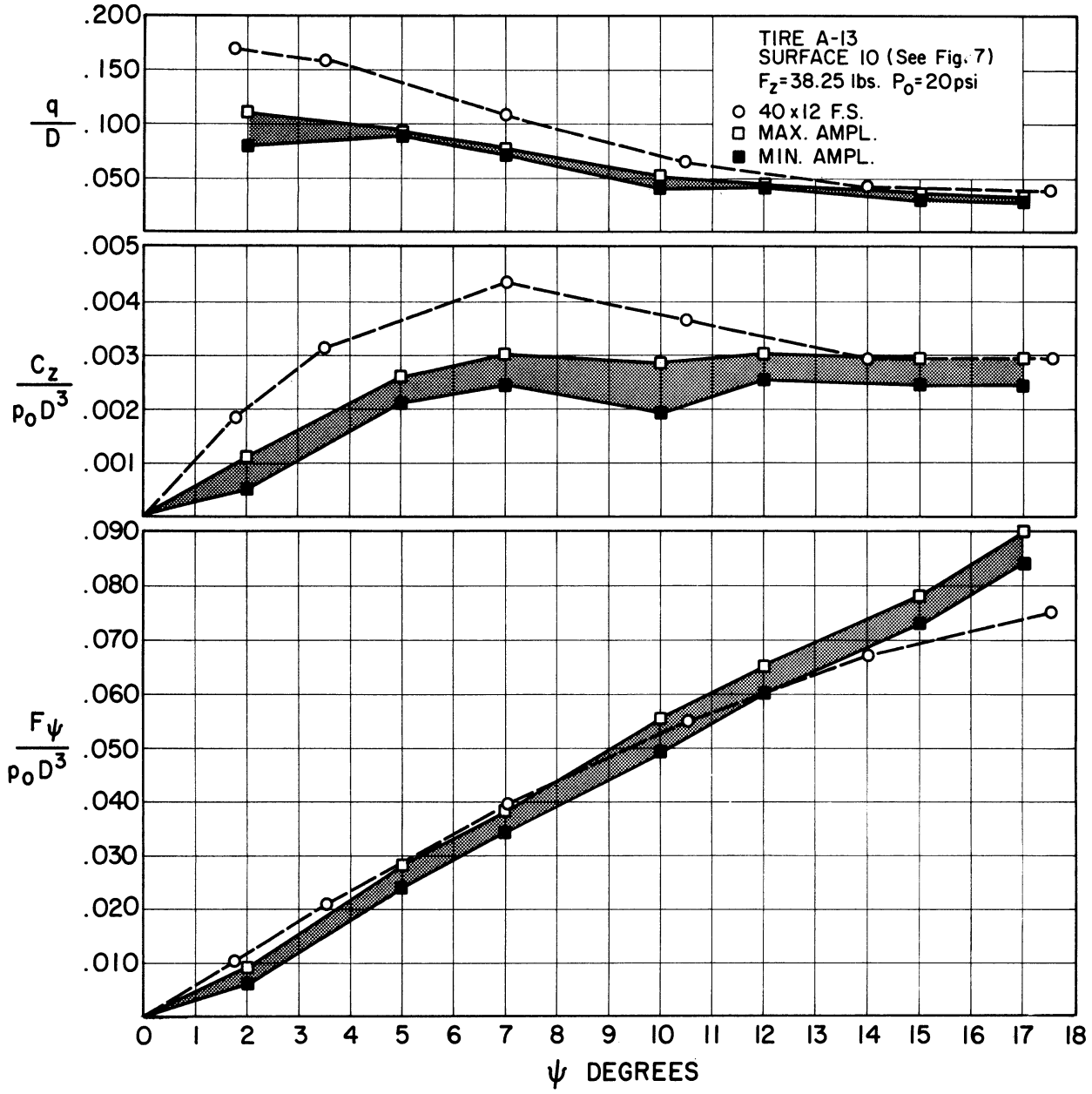

Figure 17. Variations in side force and self-aligning torque due to circumferential variations of model tire.

the circumferential side force and self-aligning torque variation for one side, while Figure 18 shows the variation in maximum amplitude from one side of the tire to the other.

Another important variation in these three slow rolling properties is due to roadwheel surface variations, as previously discussed. Many different kinds of surfaces were tried. Figure 7 shows the variation in maximum amplitude due to ten different surfaces. Rough surfaces, such as sandpaper, Safety Walk and Safety Walk coated with dental stone, gave high forces and moments at high yaw angles and tended to abrade the tires. Smooth surfaces, such as clean cast iron, Scotch Tread and Scotch Tread coated with dental stone, gave low forces and moments, but did no apparent damage to the tire. Compromise surfaces, such as Safety Walk coated with Rox and dental stone, gave the highest forces and moments which did not damage the tires. It is these smoother surfaces which were used to obtain the data in the preceding section.

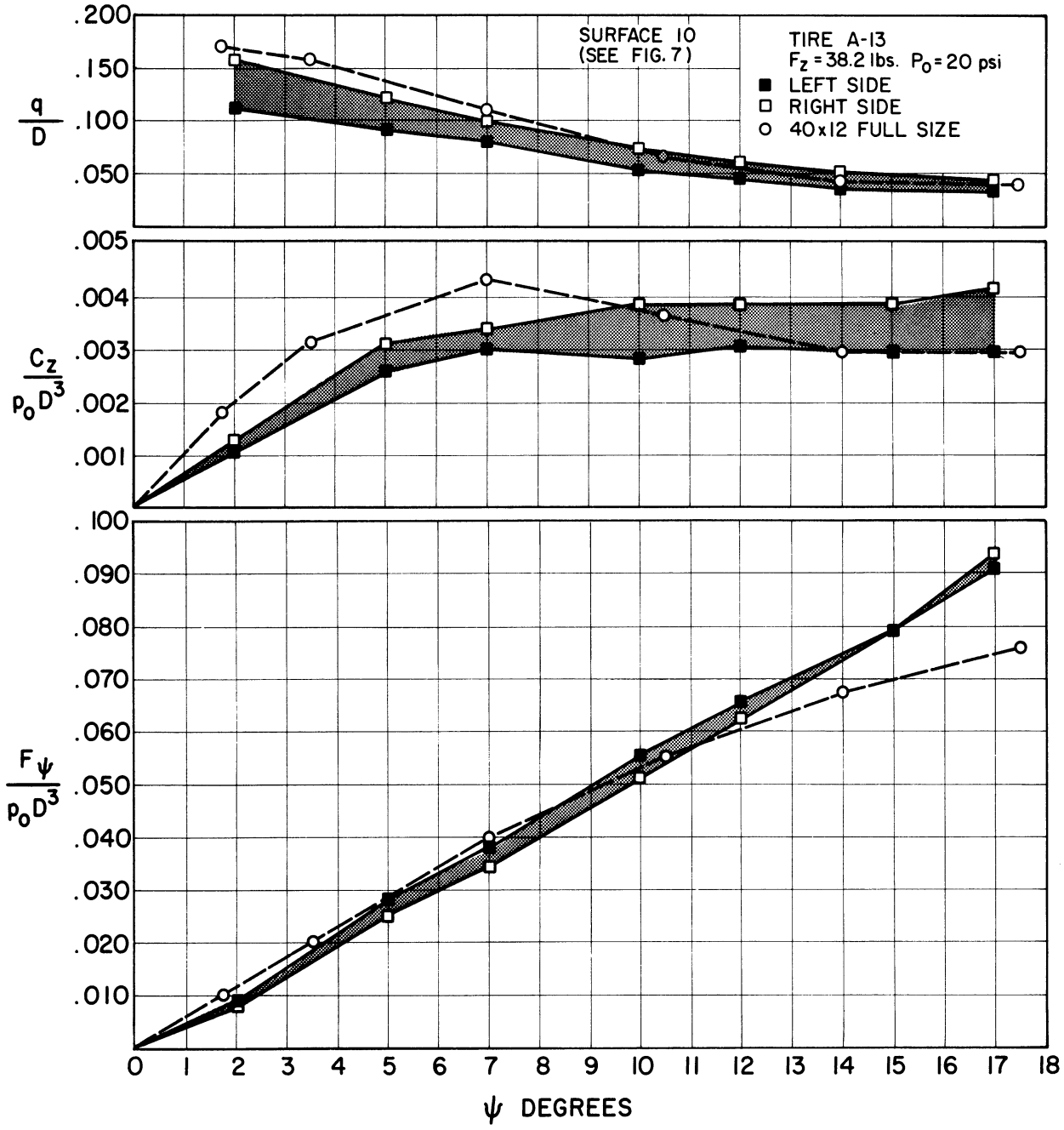

Figure 18. Variations in side force and self-aligning torque caused by side to side variations of model tire.

V. REFERENCES

1. Clark, S. K., Dodge, R. N., Lackey, J. I., and Nybakken, G. H., "Structural Modeling of Aircraft Tires," The University of Michigan, Office of Research Administration, Report 05608-16-T, May 1970, Ann Arbor, Michigan.

2. Horne, W. B., and R. F. Smiley, "Low Speed Yawed Rolling Characteristics and Other Elastic Properties of a Pair of 40 Inch Diameter 14 Ply Rating Type VII Aircraft Tires," N.A.C.A. Technical Note 4109, Washington, D.C., January 1958.

VI. DISTRIBUTION LIST

Agency	No. of Copies
Scientific and Technical Information Division Code US National Aeronautics and Space Administration Washington, D.C. 20546	25
NASA Headquarters Langley Research Center Dynamic Loads Division Hampton, Virginia 23365 Attn: Mr. Walter B. Horne	5